Supplementary information for

Diagnosing the radiation biases in global climate models using radiative kernels

Han Huang, Yi Huang

Department of Atmospheric and Oceanic Sciences, McGill University, Montreal, Canada

Corresponding Authors:

Yi Huang, yi.huang@mcgill.ca (ORCID: 0000-0002-5065-4198)

Contents of this file

Table S1-S6, as shown in the spreadsheet file "dR_globalmean_eachModel.xlsx".

Figure S1-S5

Data file: dR_globalmap_eachModel.nc

Introductions

Tables S1 and S2 show the global mean values of the total and component radiation biases in every CMIP6 GCM examined in this work. The models shown here do not include all the GCMs submitted to CMIP6, as only one model from each modelling center is (arbitrarily) selected.

Table S3 shows the standard deviation of the biases in the global mean radiation fluxes of all the models.

Tables S4 and S5 show the spatial correlation between the global distributions of the total and component radiation biases in every CMIP6 GCM.

Table S6 shows the spatial root-mean-square-error in all the latitude-longitude grid points across the globe in each model.

Figure S1 shows the biases in GCM-simulated climate variables compared to ERA5.

Figure S2 compares the model radiation biases relative to CERES and those relative to ERA5.

Figures S3 and S4 show the multi-model mean model biases in the clear-sky.

Figure S5 compares the cloud radiation biases measured by the kernel and CRE methods.

Data file "dR_globalmap_eachModel.nc" records the global distributions of radiation biases in every model.

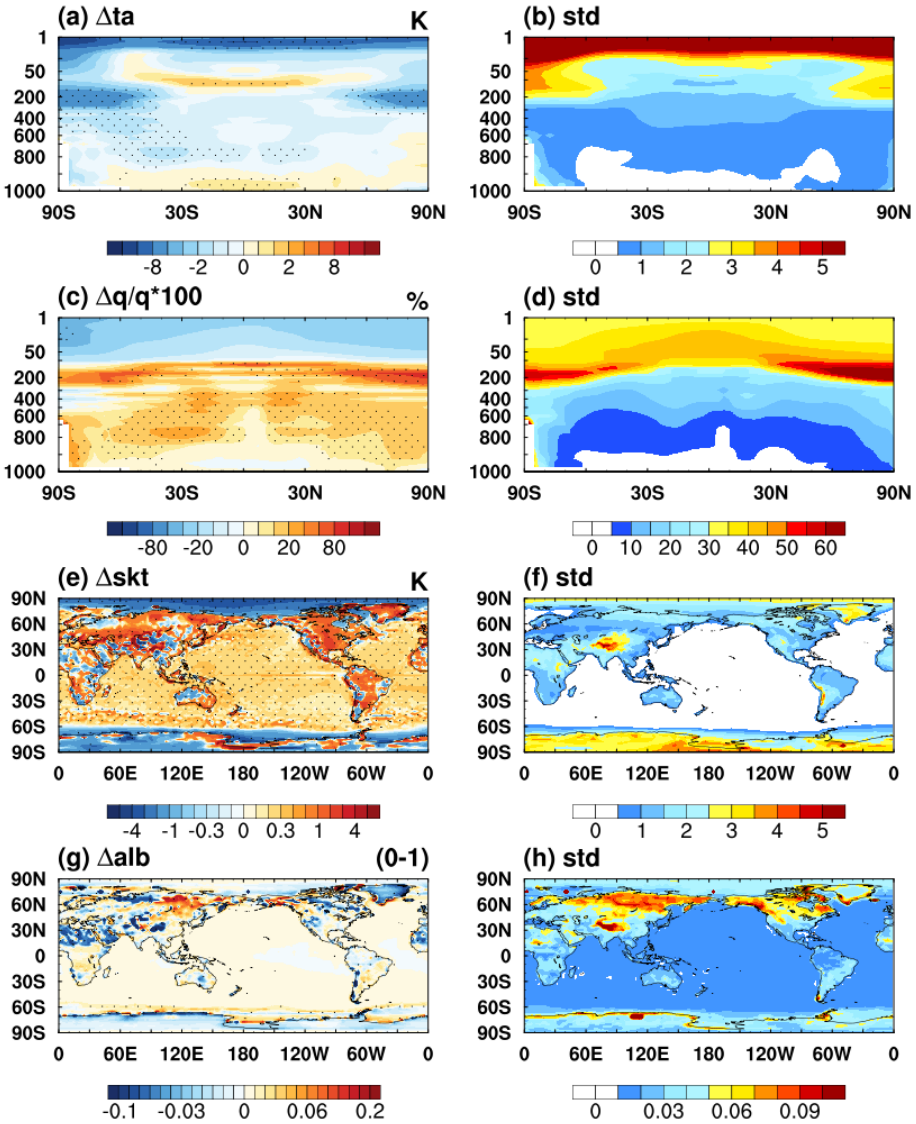

Figure S1. Multi-model mean and standard deviation (std) of the biases in modelled atmospheric variables compared to ERA5. (a, b) air temperature, units: K, (c, d) water vapor in fraction, units: %, (e, f) skin temperature, units: K, and (g, h) surface albedo. The stippled area in each panel signifies persistent biases, where the magnitude of the multi-model mean exceeds the standard deviation.

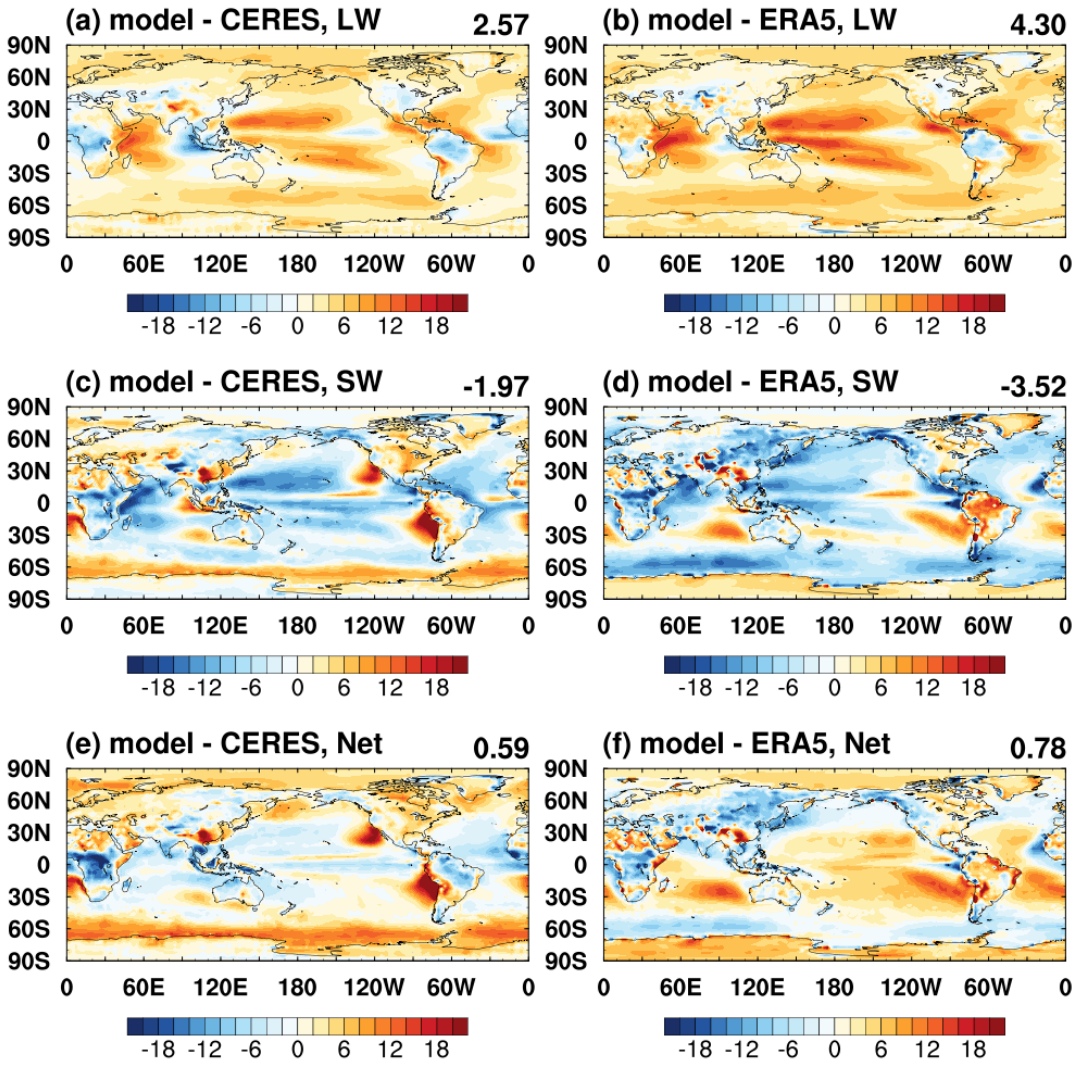

Figure S2. Multi-model mean all-sky radiation biases of the CMIP6 models compared to (a, c, e) CERES, and (b, d, f) ERA5; units: W m^{-2}. The number on the top right corner in each panel is the global mean value. The area-weighted spatial correlation between the biases relative to the two different references are: 0.80, 0.51 and 0.34 for the longwave, shortwave and net, respectively, showing their consistency.

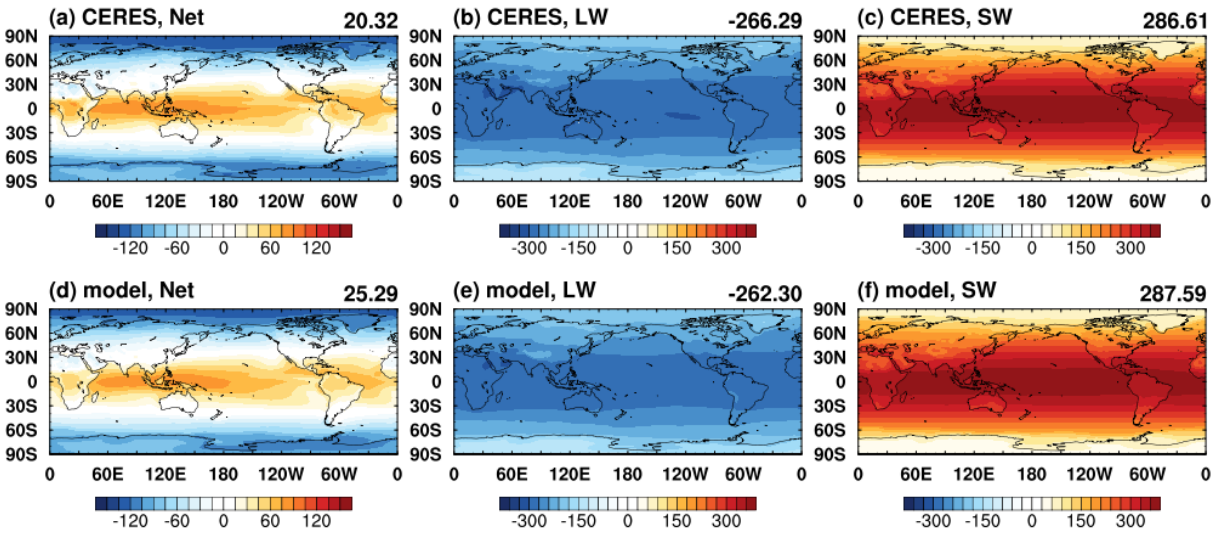

Figure S3. Like Fig. 1, but for the radiative fluxes in clear-sky (units: W m^{-2}) from (a, b, c) the CERES satellite observation, and (d, e, f) multi-model mean of the CMIP6 GCMs.

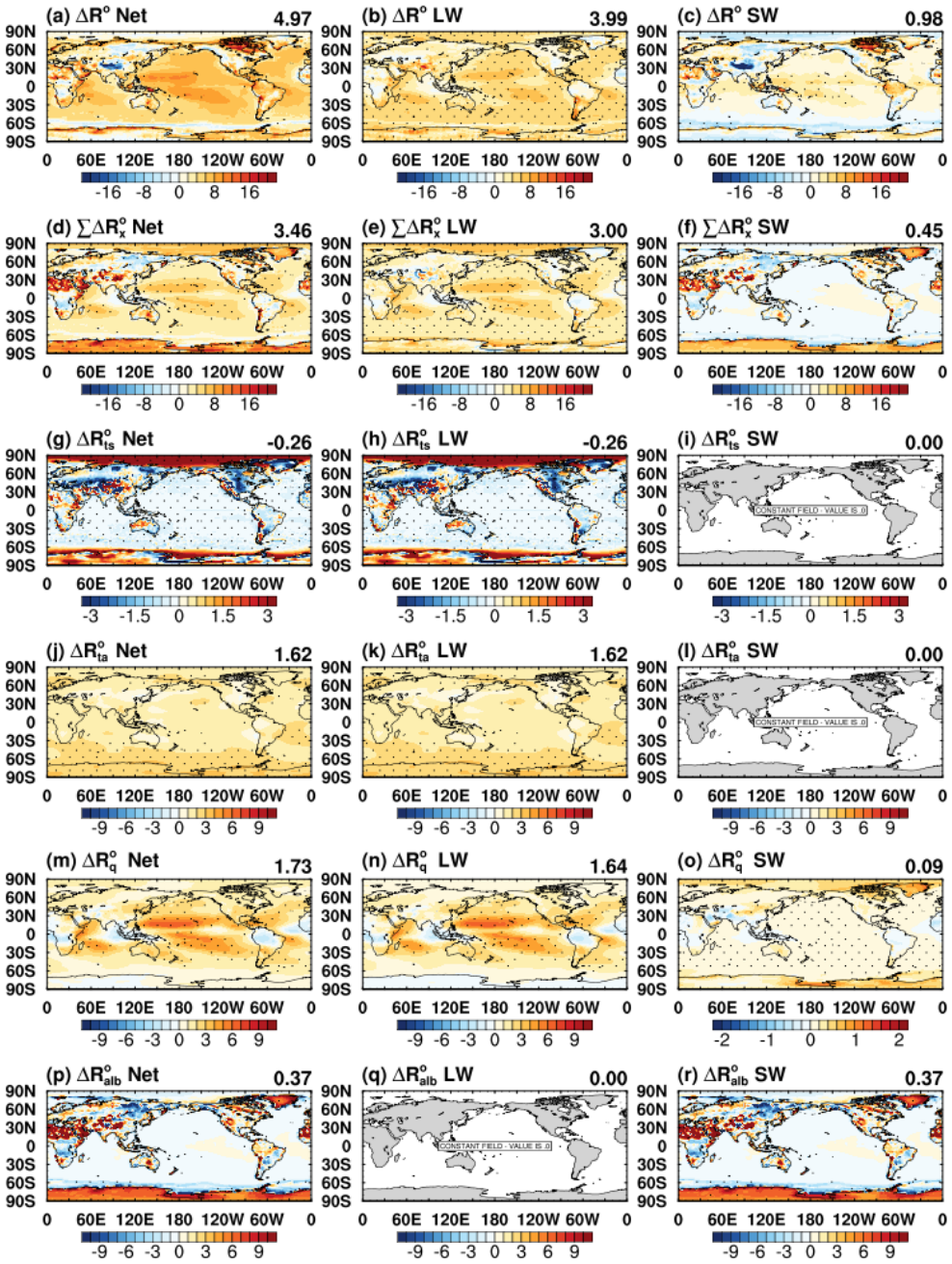

Figure S4. Similar to Fig. 3, but for the model radiation biases in the clear-sky.

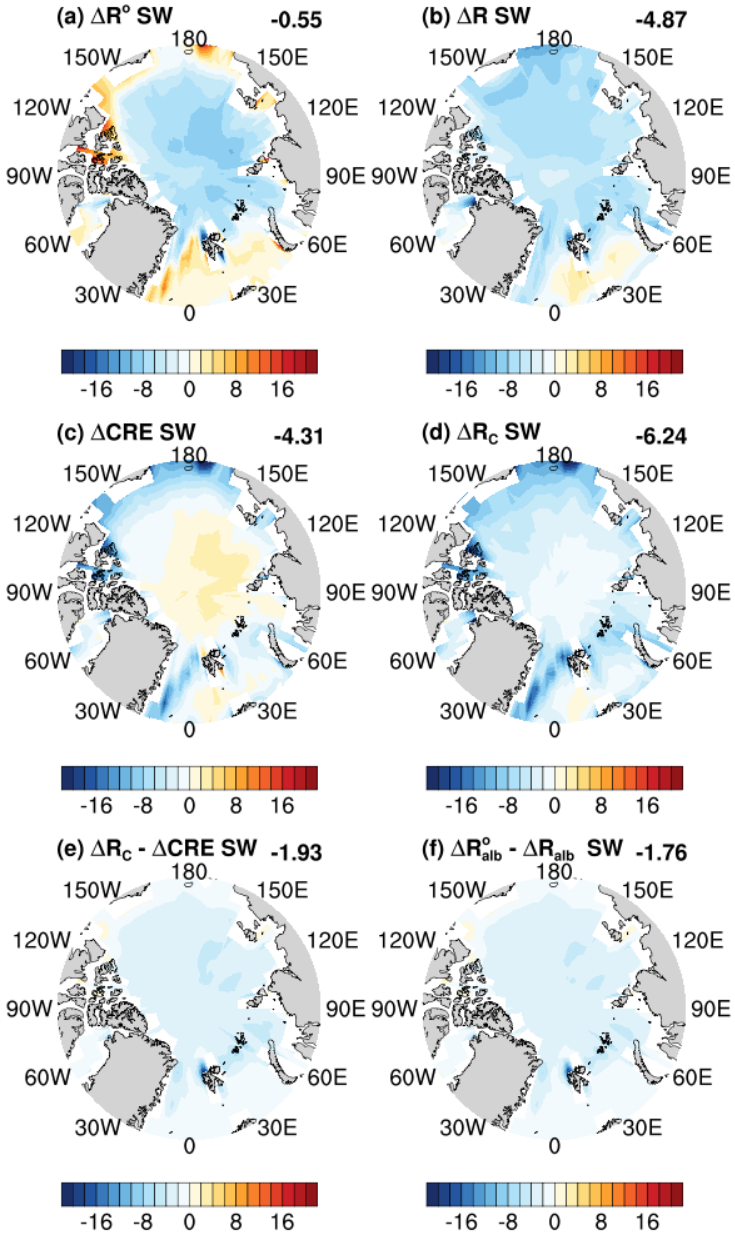

Figure S5. Comparison of cloud radiative biases measured by different methods. Shown here as an example are the radiation biases quantified for one GCM, the MPI-ESM1-2-LR model; units: W m^{-2}. (a) Clear-sky and (b) all-sky total radiation biases, and (c) their difference, i.e., cloud radiative bias measured by cloud radiative effect ΔCRE according to Equation (3). (d) Cloud radiative bias measured by the kernel method ΔR_C according to Equation (2). Their difference as shown in (e), is due to the aliasing effect caused by the surface albedo bias as shown in (f). Examining the CMIP6 GCMs one by one, we find this aliasing bias exist in a majority of the models (see the NetCDF data file documenting the component biases in the individual models).